Analytical Biochemistry 647 (2022) 114692

Contents lists available at ScienceDirect

Analytical Biochemistry

journal homepage: www.elsevier.com/locate/yabio

Formation of styrene maleic acid lipid nanoparticles (SMALPs) using SMA thin film on a substrate

Emma A. Gordon [a], Yazmyne B. Richardson [a], Muhammad Z. Shah [a], Kevin M. Burridge [a], Dominik Konkolewicz [a], Gary A. Lorigan [a,*]

[a] Department of Chemistry and Biochemistry, Miami University, Oxford, OH, 45056, USA

ARTICLE INFO

Keywords:
SMALPs
Vesicles
Transmission electron microscopy (TEM)

ABSTRACT

Despite the important role of membrane proteins in biological function and physiology, studying them remains challenging because of limited biomimetic systems for the protein to remain in its native membrane environment. Cryo electron microscopy (Cryo-EM) is emerging as a powerful tool for analyzing the structure of membrane proteins. However, Cryo-EM and other membrane protein analyses are better studied in a native lipid bilayer. Although traditional, mimetic systems have disadvantages that limit their use in the study of membrane proteins. As an alternative, styrene-maleic acid copolymers are used to form nanoparticles with POPC:POPG lipids. Traditional characterization of these styrene maleic acid lipid nanoparticles (SMALPs) includes dynamic light scattering (DLS), electron paramagnetic resonance (EPR), nuclear magnetic resonance (NMR), and transmission electron microscopy (TEM). In this study a new method was developed that utilizes SMALPs using a styrene-maleic acid copolymer (SMA) thin film on a TEM grid, acting as a substrate. By directly adding POPC: POPG lipid vesicles to the SMA coated grid SMALPs can be formed, visualized, and characterized by TEM without the need to make them in solution prior to imaging. We envision these functionalized grids could aid in single particle specimen preparation, increasing the efficiency of structural biology and biophysical techniques such as Cryo-EM.

1. Introduction

Membrane proteins are critical as they are responsible for several important biological functions, making them attractive drug targets [1,2]. Membrane proteins are challenging to study as the native lipid bilayer environment of these proteins is difficult to mimic [3,4]. Commonly used membrane mimetic systems include detergent micelles, bicelles, liposomes, and membrane scaffold protein nanodics [5–8]. Although these systems traditionally mimic the lipid bilayer and maintain the structure and function of the proteins, there are disadvantages to each system [9].

Micelles, which involve surfactant molecules forming a sphere with the hydrophobic tails facing the center leaving the hydrophilic heads on the surface, have an increased chance of protein denaturation, as well as misfolding due to mismatched hydrophobic membrane thickness [10,11]. Bicelles, bilayer micelles, are often composed of both long chain and short chain lipids that form a disk shape that allow for the study of both the hydrophobic bilayer interior as well as transmembrane proteins [12]. The disadvantage of bicelles is the limited combination of lipids that can be used to form them, limiting the range of membrane proteins that can be studied in them, as well as the possibility of protein perturbation caused by the size and shape of the bicelles [11]. Liposomes or vesicles are vesicles and can consist of multiple phospholipid lamalae [13,14]. They often have problems with solubility that can cause the protein to misfold [11]. Nanodiscs, specifically those formed via membrane scaffold proteins (MSP) wrapped around the phospholipids, allow for the stabilization of the protein [15,16]. However, the formation of these nanodiscs may require conditions that are not ideal for membrane proteins and may cause denaturation [11], and in some cases the membrane scaffold protein used to make the disc can interfere with the signal derived from the membrane protein of interest.

Several studies have used polymers to form effective biomimetic membrane nanodiscs [9,17–21]. Styrene-maleic acid copolymer lipid nanoparticles (SMALPs) have the ability to solubilize the membrane protein, without the use of detergent, while forming a narrow distribution of nanoparticles that act as a mimic of the native environment of

* Corresponding author.
E-mail address: lorigag@miamioh.edu (G.A. Lorigan).

https://doi.org/10.1016/j.ab.2022.114692
Received 4 March 2022; Received in revised form 13 April 2022; Accepted 15 April 2022
Available online 21 April 2022
0003-2697/

the protein [9,22,23]. These nanodiscs can be characterized using dynamic light scattering (DLS) [24], nuclear magnetic resonance (NMR) [25], electron paramagnetic resonance (EPR) [22], and transmission electron microscopy (TEM) [9,24,25].

Previously, TEM has been used to characterize lipid nanodiscs using a classic method involving a carbon-coated grid, vesicle:SMA complex suspended in solution, and ammonium molybdate as a negative stain [9,24,25]. TEM has also been used, in conjunction with SMALPs, to visualize membrane protein structure via Cryo-EM [26–28]. The proteins, including AcrB [26,27] and alternative complex III (ACIII) [28], were extracted from membranes by the SMA and the resulting nanodiscs were used with Cryo-EM to resolve their structure. But again, these studies use a protein/polymer complex made prior to TEM grid preparation and imaging. A problem associated with visualizing small and delicate samples with electron microscopy, such as SMALPs, is there are many steps throughout the sample preparation process that could introduce artifacts or defects that are not visible until the sample is analyzed under the microscope [29]. An effective approach to combat this is to minimize the number of steps required to prepare the sample for imaging. This study bypasses the need for the formation of the vesicle:SMA complex prior to imaging via a SMA coated TEM grid, which acts as the substrate. A SMA synthesized by RAFT polymerization [9] was used as the polymer thin film. 1-palmitoyl-2-oleoyl-glycero-3-phosphocholine and 1-palmitoyl-2-oleyl-sn-glycero-3-phospho-(1′-rac-glycerol) (POPC/POPG) vesicles were added to the TEM substrate to generate the SMALPs nanodiscs. The SMALPs were characterized by TEM and DLS.

2. Materials and methods

2.1. Vesicle preparation

Vesicle samples were composed of a 3:1 ratio of POPC and POPG. Powdered POPC and POPG lipids were dissolved in chloroform and evaporated to form a thin film on the side of a heart-shaped flask. The sample was dried overnight in a vacuum desiccator. The lipid film was suspended in a buffer containing 100 mM NaCl and 20 mM N-(2-hydroxyethyl)piperazine-*N*′-ethanesulfonic acid (HEPES) at a pH 7.0 to a final concentration of 100 mM. The solution was vortexed vigorously to mix completely and vesicles were spontaneously formed, resulting in a homogeneous milky solution after 3 freeze/sonication cycles. Vesicle solutions were then frozen with liquid nitrogen and placed in a freezer overnight (−20 °C). Any extruded vesicles were made using an Avanti mini extruder through 400 nm and 200 nm pore polycarbonate membranes at 25 °C to create different sized vesicle samples. DLS experiments were used to confirm the size of the vesicles.

2.2. SMA preparation

The synthesis of 3–1 styrene maleic acid was carried out using a previously described procedure [23]. The polymer was dissolved in a buffer containing 100 mM NaCl and 20 mM N-(2-hydroxyethyl)piperazine-*N*′-ethanesulfonic acid (HEPES) at a pH 7.0 to a final concentration of 5% m/v.

2.3. Grid preparation

Copper grids were first cleaned via sonication in acetone followed by sonication in ethanol. Grids were left to air dry at room temperature on filter paper inside a covered petri dish. A Formvar support film was then added to the grids as described previously [30]. Briefly, a clean glass slide was dipped in a 2% solution of Formvar to create a thin film. The film was then removed from the slide, floated atop a water bath, and the grids were placed on top of the film. Removal of the grids from the bath resulted in thinly coated Formvar supported grids. These grids were then carbon coated for additional support and added conductivity to the support film. The carbon coated grids were then dipped in a 5% m/v solution of SMA, blotted dry with filter paper to remove excess solution, and stored on filter paper in a covered petri dish. About 0.3 mg of polymer was left on the grid, as determined gravimetrically.

2.4. Transmission electron microscopy

All grid samples were examined in a JEOL JEM-1200EX II TEM instrument. Sample preparation, TEM imaging, and image analysis were completed at the Center for Advanced Microscopy and Imaging at Miami University.

2.5. Dynamic light scattering

DLS measurements were taken on a ZETASIZER NANO Series (Malvern Instruments) at 25 °C in 40 μL cuvettes. Data were collected in 20 s increments for 10 scans. The size distribution of the radius of the samples is shown on a log scale using MatLab.

2.6. Gramicidin A preparation

The peptide Gramicidin A was synthesized via optimized Fmoc SPSS [31]. The mutant A3C was synthesized in order to attach the spin label MTSL (S-(1-oxyl-2,2,5,5-tetramethyl-2,5-dihydro-1H-pyrrol-3-yl) methyl methanesulfonthioate) to the cysteine. Spin labeling was followed by HPLC purification and incorporation into the vesicles via a thin film method. The peptide was dissolved in DMSO:EtOH 1:1 at 0.2 mg/mL and added to predissolved vesicles in a pear shaped flask. The solvent was evaporated by N_2 gas making a uniform thin film inside the flask. It was left to dry in a desiccator overnight to remove any remaining solvent. The film was rehydrated with 10 mM phosphate buffer at 7.4 pH. Following rehydration, the solution went through 5 freeze-thaw cycles with intermittent vortexing to help maintain a homogenous mixture.

2.7. CW-EPR measurements

EPR experiments were conducted at the Ohio Advanced EPR Laboratory. CW-EPR spectra were collected at X-band on a Bruker EMX CW-EPR spectrometer using an ER041xG microwave bridge and ER4119-HS cavity coupled with a BVT 3000 nitrogen gas temperature controller. Each spin-labeled CW-EPR spectrum was acquired with a central field of 3433 G and sweep width of 150 G, modulation frequency of 100 kHz, modulation amplitude of 1 G, and microwave power of 10 mW at room temperature.

3. Results and discussion

Scheme 1 depicts the formation of the SMALPs via a SMA thin film on a TEM grid substrate. A formvar support film is first put on the copper TEM grid, followed by a carbon coating for added support and conductivity. Previously, these grids would be used to visualize SMALPs that had been formed by mixing the lipid vesicles and the SMA prior to placement on the grid [9,22–24]. The SMA polymer was synthesized by RAFT polymerization, giving a narrow molecular weight distribution [23]. The probability distribution of molecular weight of the SMA polymer is provided in Fig. S1, with a number averaged molecular weight of 11,000 and a molar mass dispersity of 1.30. A drop of the mixture would be put onto the Formvar-carbon coated grid and allowed to adsorb for several seconds before being blotted dry, stained with ammonium molybdate, and then imaged in the TEM. It is during these steps that often times artifacts from the stain will adhere to the grid or there will be damage caused to the support film itself due to over-handling of the grid [29]. These artifacts can include mechanical, chemical, or physical damage caused by a preparation technique and can be confused for microstructure in the sample [32].

In this study, the Formvar-carbon coated grids were additionally

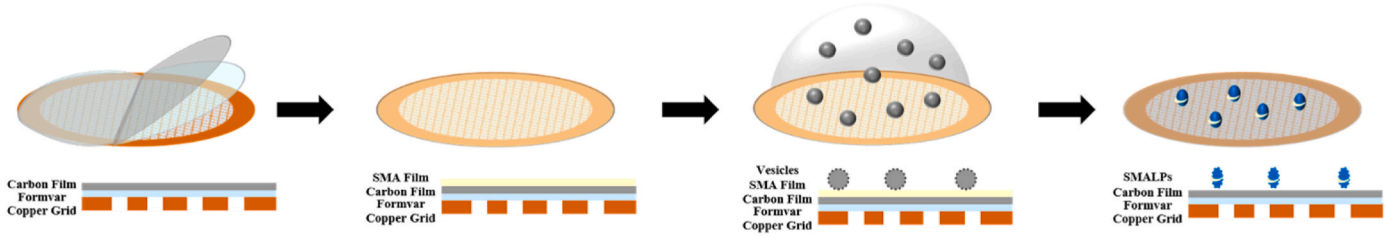

Scheme 1. Workflow of preparing the SMALPs for TEM imaging using a grid prepared with a SMA thin film.

coated with the SMA polymer, creating a thin film atop the Formvar and carbon layers. Once dry, the SMA coated grids were then used to form and image the SMALPs. A drop of lipid POPC:POPG vesicle solution was placed on the grid and left for several seconds to allow for both the formation of the SMALPs, as well as their adsorbance onto the grid. The droplet of lipid vesicles rehydrates the dried SMA film on the grid and it is then able to form the nanodiscs. At this point it is ready to be imaged under the TEM. By using a grid with the SMA thin film, there is a reduction in the possibility for sample damage and interfering artifacts to appear in the TEM images as it is a single step sample preparation process.

Dynamic light scattering is a common way to characterize the size of both lipid vesicles and SMALPs [9,23,24]. Fig. 1A shows the DLS data for POPC:POPG vesicles and SMALPs generated from a lipid:SMA ratio of 1:1.5 v/v. The average radius size of the POPC:POPG vesicles was 700 nm, and the average radius size of the vesicle:SMA nanodisc was 16 nm. This is shown by the unimodal peak with a wide distribution indicating heterogeneity in the size of the sample. Previous studies have shown similar results using both POPC vesicles [22,23] and various ratios of POPC:POPG vesicles [24]. In these studies, the SMALPs were found to have a homogeneous size distribution despite the various lipid compositions, also characterized by DLS. Previous work has also shown that the size of these SMALPs can be varied based on the St:MA ratio of the polymer [9]. It was found that the size of the nanodisc is independent of the molecular weight of the polymer but rather is dependent on the St:MA ratio, confirmed by DLS and TEM. Fig. 1B is a TEM image of the POPC vesicles on a traditional Formvar-carbon coated TEM grid. The size, as estimated by the scale bar, is consistent with the DLS data. Similarly, a droplet of the POPC:POPG vesicles was placed on a TEM grid layered with the SMA film, the resulting TEM image of the SMALPs is shown in Fig. 1C. The estimated diameter, via scale bar, is 30 nm which matches well with the DLS data for the SMALPs generated from the vesicle:SMA nanodiscs. This agreement in size shows that the use of the SMA coated TEM grid to form and characterize SMALPs is equally as effective to the traditional method of forming SMALPs in solution prior to visualization.

Extruded vesicles were also used to confirm the effectiveness of the thin film. Fig. 2A/D. shows the DLS data for POPC vesicles extruded using a 200 nm and a 400 nm pore polycarbonate membrane. The corresponding TEM images of these vesicles are shown in Fig. 2B and E. These extruded vesicles were put on a TEM grid layered with the SMA film. The corresponding TEM images can be seen in Fig. 2C and F. The estimated diameter of the SMALPs formed on the grid by using both the 400 nm extruded vesicles, as well as the 200 nm extruded vesicles, is 40 nm which agrees with the DLS data for the SMALPs generated from the extruded vesicles and SMA in solution.

SMALPs that were formed on the TEM grid were also characterized using DLS, as shown in Fig. 3. An initial DLS spectra was taken of the POPC vesicles (black), and then the vesicles were put onto a TEM grid with the SMA film to form the SMALPs. After formation, the SMALPs were rinsed off the grid and characterized with DLS (blue). For comparison, a solution of SMALPs was also made via a mixture of 1:1.5 v/v lipid:SMA and then characterized by DLS (red). The characterization of both the SMALPs formed via the SMA thin film and the mixture of 1:1.5 v/v lipid:SMA by DLS agree.

In order to determine the lifetime of the SMA film on the TEM grids, the grids were allowed to age between 0 and 60 days. Fig. 4A shows the TEM images day 0, 7, 28, and 60. Grids were incubated under ambient laboratory conditions for the specified amount of time and then on the day of imaging, vesicles were added to the grids. Subsequently, the resulting SMALPs were analyzed by TEM to examine their shelf life. The surface morphology of the aging film was also investigated via SEM to check for cracks or defects that may have form over time. This data can be seen in Fig. S2.

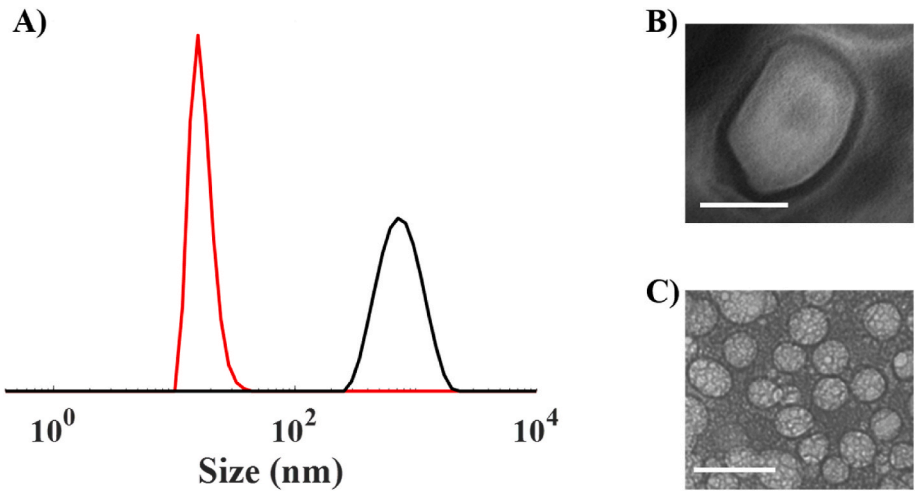

Fig. 1. A) Size distribution of 3:1 POPC:POPG vesicles (black) and SMALPs generated from a lipid:SMA ratio of 1:5 v/v (red). TEM micrographs of **B)** 3:1 POPC:POPG vesicles; scale bar = 500 nm and **C)** SMALPs generated via SMA thin film; scale bar = 50 nm. (For interpretation of the references to colour in this figure legend, the reader is referred to the Web version of this article.)

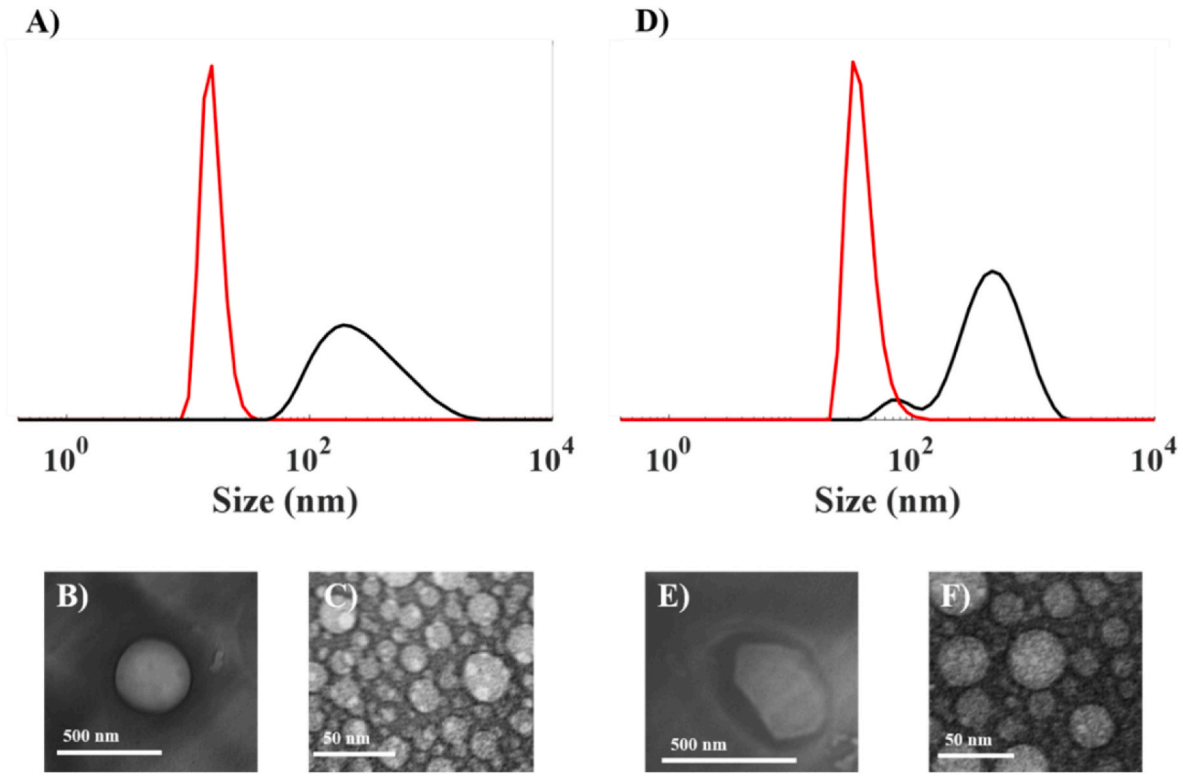

Fig. 2. **A)** Size distribution of 200 nm extruded vesicles (black) and the SMALPs generated by these vesicles and SMA in a 1:1.5 ratio v/v (red). TEM micrographs of **B)** extruded vesicles and **C)** SMALPs formed with the extruded vesicles via SMA thin film. **D)** Size distribution of 400 nm extruded vesicles (black) and the SMALPs generated by these vesicles and SMA in a 1:1.5 ratio v/v (red). TEM micrographs of **E)** extruded vesicles and **F)** SMALPs formed with the extruded vesicles via SMA thin film. (For interpretation of the references to colour in this figure legend, the reader is referred to the Web version of this article.)

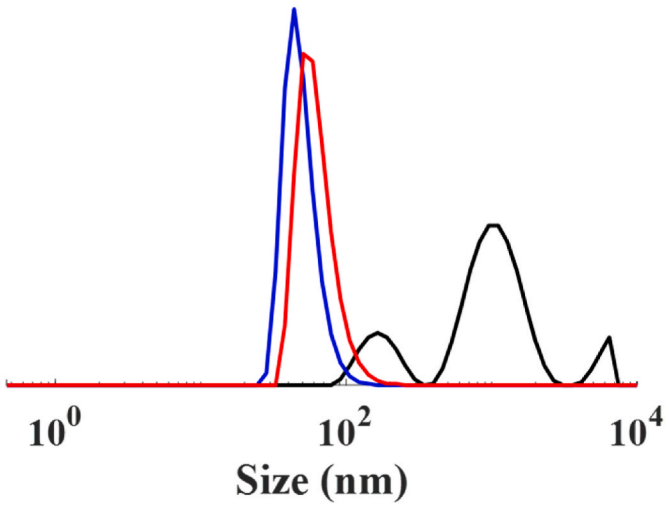

Fig. 3. Size distribution of 3:1 POPC:POPG vesicles (black), SMALPs generated from a lipid:SMA ratio of 1:5 v/v (red), and SMALPs formed on a TEM grid via the SMA thin film (blue). (For interpretation of the references to colour in this figure legend, the reader is referred to the Web version of this article.)

The images taken of the vesicles on the aged SMA TEM film grids were analyzed using Image J (Java) to determine the average size of the SMALPs and to determine if that size changed as the film aged [33]. A histogram of the size distribution of each age is shown in Fig. 4B, n = 100 SMALPs. The distribution of SMALPs size stays relatively consistent over the 60 days with only minor changes in the size distribution, suggesting that aging does not affect the efficacy of the SMA film. It also suggests that if these grids are prepared ahead of experimentation the shelf life would be at least two months.

To test the compatibility of the SMA substrate with membrane proteins, the model membrane protein Gramicidin A was incorporated into 3:1 POPC:POPG vesicles. In order to show the protein remains incorporated after the formation of SMALPs, A3C Gramicidin A was spin labeled and incorporated into 3:1 POPC:POPG vesicles as well as formed into SMALPs by addition of 1:1.5 v/v SMA. CW-EPR spectra can be seen for both the vesicles and the nanodiscs in Fig. 5A. The spin-labeled Gramicidin A in the SMALP system showed line broadening, which is consistent with previous work with membrane proteins and nanodiscs [24,34]. Dynamic light scattering was used to characterize the SMALPs with incorporated Gramicidin A that were formed in solution as well as formed on the TEM grid substrate. Fig. 5B shows the DLS spectra for POPC:POPG vesicles with incorporated Gramicidin A (black), SMALPs formed in solution (red), and the SMALPs formed on the grid (blue). The average size of the nanodiscs were 20 nm, which is consistent with what was seen in the TEM micrograph shown in Fig. 5C, as well as what was observed in vesicles that had no incorporated protein.

4. Conclusion

The use of SMALPs in membrane protein studies is growing and as a result so is the importance of characterization [22,24,25,35–39]. In this study, SMALPs were characterized by TEM using a SMA coated TEM grid substrate. The size of the SMALPs seen on the TEM grid were essentially the same as the SMALPs formed in solution, as is traditionally done. This suggests that using the SMA thin film as a new TEM grid support for forming and imaging SMALPs is comparable to the traditional method of characterization by way of forming lipid:SMA nanodiscs in solution. This technique has potential applications in more complex protein biophysical and imaging techniques, such as Cryo-EM.

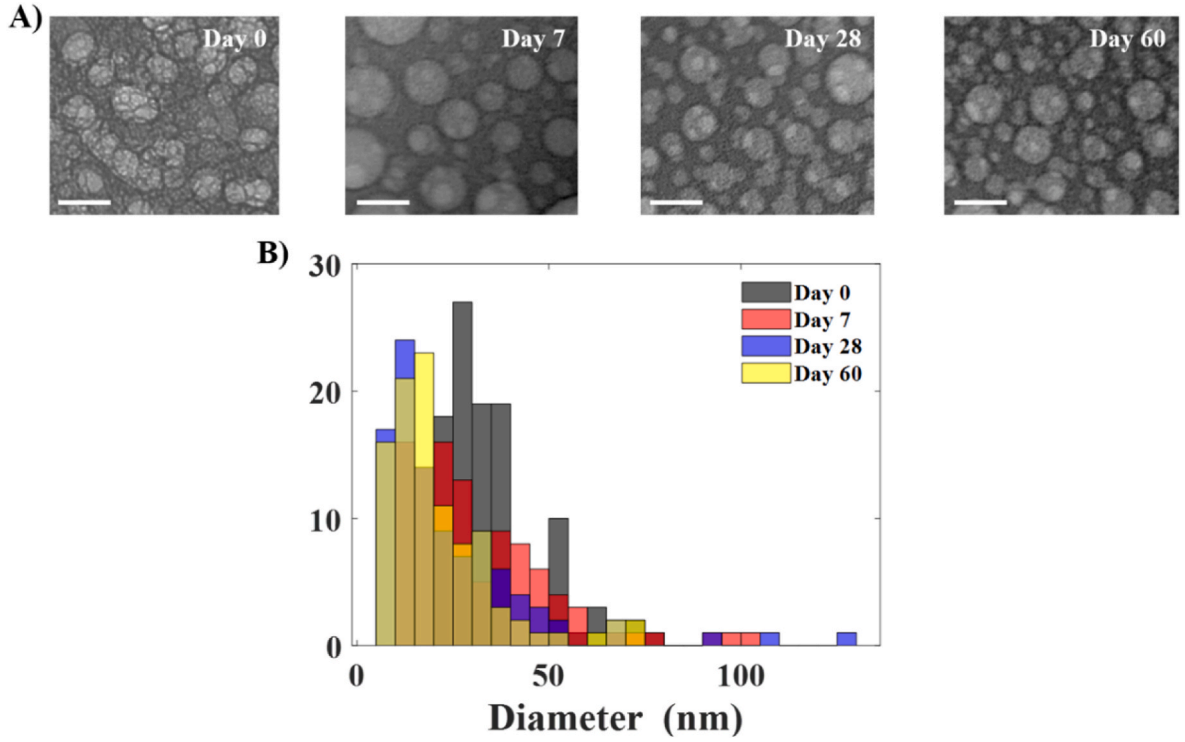

Fig. 4. **A)** TEM micrographs of SMALPs formed on aged SMA thin film TEM grids; scale bar = 50 nm. **B)** Histogram showing the distribution of the size of the SMALPs as the thin film is aged; n = 100.

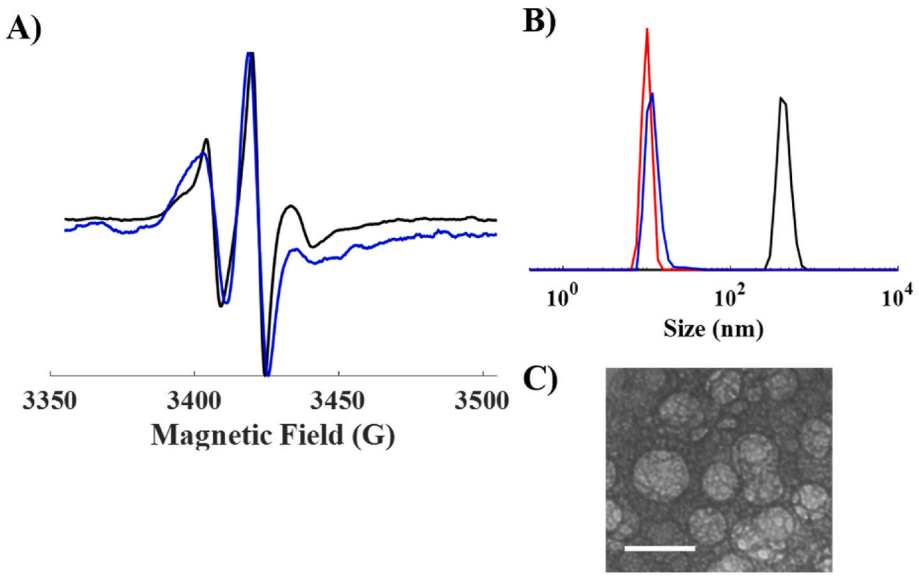

Fig. 5. **A)** CW-EPR data on A3C spin-labeled Gramicidin A in 3:1 POPC:POPG vesicles (black) and SMALPs formed from 1:1.5 v/v lipid:SMA (blue) **B)** Size distribution of 3:1 POPC:POPG vesicles containing Gramicidin A (black), SMALPs generated from a lipid:SMA ratio of 1:5 v/v (red), and SMALPs formed on a TEM grid via the SMA thin film (blue). **C)** TEM micrographs of SMALPs formed on aged SMA thin film TEM grids; scale bar = 50 nm. (For interpretation of the references to colour in this figure legend, the reader is referred to the Web version of this article.)

CRediT author statement

Emma A. Gordon: Conceptualization, Methodology, Investigation, Formal analysis, Writing – original draft. **Yazmyne B. Richardson:** Investigation. **Muhammad Z. Shah:** Investigation. **Kevin M. Burridge:** Investigation. **Dominik Konkolewicz:** Supervision, Writing – review & editing. **Gary A. Lorigan:** Project administration, Funding acquisition, Supervision, Writing – review & editing.

Declarations of competing interest

None.

Acknowledgements

This work was generously supported by an NIGMS/NIH Maximizing Investigator's Research Award (MIRA) R35 GM126935 grant to G.A.L. Dr. Dominik Konkolewicz acknowledges support from Miami University through the Robert H and Nancy J Blayney Professorship.

Appendix A. Supplementary data

Supplementary data to this article can be found online at https://doi.org/10.1016/j.ab.2022.114692.

References

[1] H. Yin, A.D. Flynn, Drugging membrane protein interactions, Annu. Rev. Biomed. Eng. 18 (1) (2016) 51–76, https://doi.org/10.1146/annurev-bioeng-092115-025322.

[2] C. Zheng, L. Han, C.W. Yap, B. Xie, Y. Chen, Progress and problems in the exploration of therapeutic targets, Drug Discov. Today 11 (9) (2006) 412–420, https://doi.org/10.1016/j.drudis.2006.03.012.

[3] J.N. Sachs, D.M. Engelman, Introduction to the membrane protein reviews: the interplay of structure, dynamics, and environment in membrane protein function, Annu. Rev. Biochem. 75 (1) (2006) 707–712, https://doi.org/10.1146/annurev.biochem.75.110105.142336.

[4] C.G. Tate, Practical considerations of membrane protein instability during purification and crystallisation, Methods Mol. Biol. Clifton NJ 601 (2010) 187–203, https://doi.org/10.1007/978-1-60761-344-2_12.

[5] A.M. Seddon, P. Curnow, P.J. Booth, Membrane proteins, lipids and detergents: not just a soap opera, Biochim. Biophys. Acta BBA - Biomembr. 1666 (1) (2004) 105–117, https://doi.org/10.1016/j.bbamem.2004.04.011.

[6] T.H. Bayburt, S.G. Sligar, Membrane protein assembly into nanodiscs, FEBS Lett. 584 (9) (2010) 1721–1727, https://doi.org/10.1016/j.febslet.2009.10.024.

[7] Self-assembly of Single Integral Membrane Proteins into Soluble Nanoscale Phospholipid Bilayers - Bayburt - 2003 - Protein Science - Wiley Online Library https://onlinelibrary.wiley.com/doi/full/10.1110/ps.03267503 (accessed 2022 -01 -03).

[8] J. Dorr, S. Scheidelaar, M. Koorengevel, J. Dominguez, M. Schafer, C. Van Walree, J. Killian, The styrene–maleic acid copolymer: a versatile tool in membrane Research, Eur. Biophys. J. Biophys. Lett. 45 (1) (2016) 3–21, https://doi.org/10.1007/s00249-015-1093-y.

[9] A.F. Craig, E.E. Clark, I.D. Sahu, R. Zhang, N.D. Frantz, M.S. Al-Abdul-Wahid, C. Dabney-Smith, D. Konkolewicz, G.A. Lorigan, Tuning the size of styrene-maleic acid copolymer-lipid nanoparticles (SMALPs) using RAFT polymerization for biophysical studies, Biochim. Biophys. Acta BBA - Biomembr. 1858 (11) (2016) 2931–2939, https://doi.org/10.1016/j.bbamem.2016.08.004.

[10] R.M. Garavito, S. Ferguson-Miller, Detergents as tools in membrane biochemistry, J. Biol. Chem. 276 (35) (2001) 32403–32406, https://doi.org/10.1074/jbc.R100031200.

[11] S. Majeed, A.B. Ahmad, U. Sehar, E.R. Georgieva, Lipid membrane mimetics in functional and structural studies of integral membrane proteins, Membranes 11 (9) (2021) 685, https://doi.org/10.3390/membranes11090685.

[12] C.R. Sanders, R.S. Prosser, Bicelles: a model membrane system for all seasons? Structure 6 (10) (1998) 1227–1234, https://doi.org/10.1016/S0969-2126(98)00123-3.

[13] A. Akbarzadeh, R. Rezaei-Sadabady, S. Davaran, S.W. Joo, N. Zarghami, Y. Hanifehpour, M. Samiei, M. Kouhi, K. Nejati-Koshki, Liposome: classification, preparation, and applications, Nanoscale Res. Lett. 8 (1) (2013) 102, https://doi.org/10.1186/1556-276X-8-102.

[14] J.C. Bozelli, S.S. Aulakh, R.M. Epand, Membrane shape as determinant of protein properties, Biophys. Chem. 273 (2021), 106587, https://doi.org/10.1016/j.bpc.2021.106587.

[15] I.G. Denisov, S.G. Sligar, Nanodiscs for structural and functional studies of membrane proteins, Nat. Struct. Mol. Biol. 23 (6) (2016) 481–486, https://doi.org/10.1038/nsmb.3195.

[16] S. Damiati, A. Scheberl, S. Zayni, S.A. Damiati, B. Schuster, U.B. Kompella, Albumin-bound nanodiscs as delivery vehicle candidates: development and characterization, Biophys. Chem. 251 (2019) 106178, https://doi.org/10.1016/j.bpc.2019.106178.

[17] T. Ravula, N.Z. Hardin, S.K. Ramadugu, S.J. Cox, A. Ramamoorthy, formation of PH-resistant monodispersed polymer–lipid nanodiscs, Angew. Chem. Int. Ed. 57 (5) (2018) 1342–1345, https://doi.org/10.1002/anie.201712017.

[18] E.R. Geertsma, N.a.B. Nik Mahmood, G.K. Schuurman-Wolters, B. Poolman, Membrane reconstitution of ABC transporters and assays of translocator function, Nat. Protoc. 3 (2) (2008) 256–266, https://doi.org/10.1038/nprot.2007.519.

[19] G. Fang, R. Friesen, F. Lanfermeijer, A. Hagting, B. Poolman, W.N. Konings, Manipulation of activity and orientation of membrane-reconstituted di-tripeptide transport protein DtpT of lactococcus lactis, Mol. Membr. Biol. 16 (4) (1999) 297–304, https://doi.org/10.1080/096876899294517.

[20] F. Hagn, M. Etzkorn, T. Raschle, G. Wagner, Optimized phospholipid bilayer nanodiscs facilitate high-resolution structure determination of membrane proteins, J. Am. Chem. Soc. 135 (5) (2013) 1919–1925, https://doi.org/10.1021/ja310901f.

[21] R.R. Vold, R.S. Prosser, Magnetically oriented phospholipid bilayered micelles for structural studies of polypeptides. Does the ideal bicelle exist? J. Magn. Reson. 113 (1996) 267–271, https://doi.org/10.1006/jmrb.1996.0187.

[22] A.P. Bali, I.D. Sahu, A.F. Craig, E.E. Clark, K.M. Burridge, M.T. Dolan, C. Dabney-Smith, D. Konkolewicz, G.A. Lorigan, Structural characterization of styrene-maleic acid copolymer-lipid nanoparticles (SMALPs) using EPR spectroscopy, Chem. Phys. Lipids 220 (2019) 6–13, https://doi.org/10.1016/j.chemphyslip.2019.02.003.

[23] K.M. Burridge, B.D. Harding, I.D. Sahu, M.M. Kearns, R.B. Stowe, M.T. Dolan, R. E. Edelmann, C. Dabney-Smith, R.C. Page, D. Konkolewicz, G.A. Lorigan, Simple derivatization of RAFT-synthesized styrene–maleic anhydride copolymers for lipid disk formulations, Biomacromolecules 21 (3) (2020) 1274–1284, https://doi.org/10.1021/acs.biomac.0c00041.

[24] B.D. Harding, G. Dixit, K.M. Burridge, I.D. Sahu, C. Dabney-Smith, R.E. Edelmann, D. Konkolewicz, G.A. Lorigan, Characterizing the structure of styrene-maleic acid copolymer-lipid nanoparticles (SMALPs) using RAFT polymerization for membrane protein spectroscopic studies, Chem. Phys. Lipids 218 (2019) 65–72, https://doi.org/10.1016/j.chemphyslip.2018.12.002.

[25] R. Zhang, I.D. Sahu, L. Liu, A. Osatuke, R.G. Comer, C. Dabney-Smith, G.A. Lorigan, Characterizing the structure of lipodisq nanoparticles for membrane protein spectroscopic studies, Biochim. Biophys. Acta BBA - Biomembr. 1848 (1) (2015) 329–333, https://doi.org/10.1016/j.bbamem.2014.05.008. Part B).

[26] M. Parmar, S. Rawson, C.A. Scarff, A. Goldman, T.R. Dafforn, S.P. Muench, V.L. G. Postis, Using a SMALP platform to determine a sub-nm single particle cryo-EM membrane protein structure, Biochim. Biophys. Acta BBA - Biomembr. 1860 (2) (2018) 378–383, https://doi.org/10.1016/j.bbamem.2017.10.005.

[27] W. Qiu, Z. Fu, G.G. Xu, R.A. Grassucci, Y. Zhang, J. Frank, W.A. Hendrickson, Y. Guo, Structure and activity of lipid bilayer within a membrane-protein transporter, Proc. Natl. Acad. Sci. Unit. States Am. 115 (51) (2018) 12985–12990, https://doi.org/10.1073/pnas.1812526115.

[28] C. Sun, S. Benlekbir, P. Venkatakrishnan, Y. Wang, S. Hong, J. Hosler, E. Tajkhorshid, J.L. Rubinstein, R.B. Gennis, Structure of the alternative complex III in a supercomplex with cytochrome oxidase, Nature 557 (7703) (2018) 123–126, https://doi.org/10.1038/s41586-018-0061-y.

[29] J. Kuo (Ed.), Electron Microscopy: Methods and Protocols, third ed.Methods in Molecular Biology, Humana Press, New York, 2014.

[30] J.J. Bozzola, L.D. Russell, Electron Microscopy: Principles and Techniques for Biologists, second ed., Jones and Bartlett, Sudbury, Mass, 1999.

[31] T. Ahammad, D.L. Drew, I.D. Sahu, R.A. Serafin, K.R. Clowes, G.A. Lorigan, Continuous wave electron paramagnetic resonance spectroscopy reveals the structural topology and dynamic properties of active pinholin S2168 in a lipid bilayer, J. Phys. Chem. B 123 (38) (2019) 8048–8056, https://doi.org/10.1021/acs.jpcb.9b06480.

[32] J. Ayache, L. Beaunier, J. Boumendil, G. Ehret, D. Laub, Artifacts in transmission electron microscopy, in: J. Ayache, L. Beaunier, J. Boumendil, G. Ehret, D. Laub (Eds.), Sample Preparation Handbook for Transmission Electron Microscopy: Methodology, Springer, New York, NY, 2010, pp. 125–170, https://doi.org/10.1007/978-0-387-98182-6_6.

[33] C.A. Schneider, W.S. Rasband, K.W. Eliceiri, NIH image to ImageJ: 25 Years of image analysis, Nat. Methods 9 (7) (2012) 671–675, https://doi.org/10.1038/nmeth.2089.

[34] I.D. Sahu, R. Zhang, M.M. Dunagan, A.F. Craig, G.A. Lorigan, Characterization of KCNE1 inside lipodisq nanoparticles for EPR spectroscopic studies of membrane proteins, J. Phys. Chem. B 121 (21) (2017) 5312–5321, https://doi.org/10.1021/acs.jpcb.7b01705.

[35] T. Ravula, N.Z. Hardin, A. Ramamoorthy, Polymer nanodiscs: advantages and limitations, Chem. Phys. Lipids 219 (2019) 45–49, https://doi.org/10.1016/j.chemphyslip.2019.01.010.

[36] D. Beriashvili, N.R. Spencer, T. Dieckmann, M. Overduin, M. Palmer, Characterization of multimeric daptomycin bound to lipid nanodiscs formed by calcium-tolerant styrene-maleic acid copolymer, Biochim. Biophys. Acta BBA - Biomembr. 1862 (6) (2020), 183234, https://doi.org/10.1016/j.bbamem.2020.183234.

[37] T. Ravula, S.K. Ramadugu, G. Di Mauro, A. Ramamoorthy, Bioinspired, size-tunable self-assembly of polymer–lipid bilayer nanodiscs, Angew. Chem. 129 (38) (2017) 11624–11628, https://doi.org/10.1002/ange.201705569.

[38] M. Hoffmann, J. Eisermann, F.A. Schöffmann, M. Das, C. Vargas, S. Keller, D. Hinderberger, Influence of Different Polymer Belts on Lipid Properties in Nanodiscs Characterized by CW EPR Spectroscopy. https://doi.org/10.26434/chemrxiv.14398259.v1, 2021.

[39] I.D. Sahu, G. Dixit, W.D. Reynolds, R. Kaplevatsky, B.D. Harding, C.K. Jaycox, R. M. McCarrick, G.A. Lorigan, Characterization of the human KCNQ1 voltage sensing domain (VSD) in lipodisq nanoparticles for electron paramagnetic resonance (EPR) spectroscopic studies of membrane proteins, J. Phys. Chem. B 124 (12) (2020) 2331–2342, https://doi.org/10.1021/acs.jpcb.9b11506.